Am J Nucl Med Mol Imaging 2025;15(1):1-14
www.ajnmmi.us /ISSN:2160-8407/ajnmmi0163505

Review Article

Research process of PET tracers for neuroendocrine tumors diagnosis

Xiangyuan Bao[1,2], Shuai Li[1], Shaobo Yao[1,2], Qiusong Chen[1]

[1]Department of PET/CT Diagnostic, Tianjin Key Lab of Functional Imaging and Tianjin Institute of Radiology, Tianjin Medical University General Hospital, Tianjin 300052, China; [2]The Clinical Research and Translational Center, The First Affiliated Hospital of Fujian Medical University, Fuzhou 350005, Fujian, China

Received January 22, 2025; Accepted February 14, 2025; Epub February 25, 2025; Published February 28, 2025

Abstract: Neuroendocrine tumors (NETs) can affect several organ systems and present a variety of clinical symptoms, which are difficult to diagnose by conventional methods. Somatostatin receptor (SSTR) is a group of specific receptors expressed on the well-differentiated NET cell membrane. [^{68}Ga]-labeled somatostatin analogues (SSAs) PET/CT, endogenous ligands targeting SSTR, is widely used in currently clinical NETs diagnosis. The dual-tracer strategy ([^{68}Ga]Ga-SSAs + [^{18}F]FDG) allows for a more detailed evaluation of tumor metabolism and receptor expression. The NETPET score, integrating [^{68}Ga]Ga-SSAs PET/CT and [^{18}F]FDG PET/CT results, enhances the accuracy of predicting treatment response and prognosis. In addition, novel isotopes ([^{18}F]/[^{64}Cu]) labeled SSAs and SSTR antagonists outperformed [^{68}Ga]-SSAs in lesion detection, tumor uptake, and tumor-to-background ratio. Due to undifferentiated or dedifferentiated NETs, SSTR may not be expressed. [^{68}Ga]Ga-Pentixafor and [^{18}F]-FDG PET/CT are applicable for SSTR-negative NET diagnosis. [^{18}F]-MFBG and [^{18}F]-DOPA have a higher sensitivity for identifying non-metastatic pheochromocytoma and paraganglioma (PPGL) than other radiotracers. This review addressed NET diagnosis with conventional imaging techniques, the clinical application of novel radiotracers, and the merits and limitations of the various radiotracers.

Keywords: Somatostatin receptor, PET/CT, radiotracer, neuroendocrine tumors

Introduction

Neuroendocrine cells from the gastrointestinal or bronchopulmonary systems are the most common source of neuroendocrine tumors (NETs) [1]. As a result of better techniques for detecting tumors, the incidence and frequency of NETs have increased globally [2]. NETs are rare, heterogeneous, and typically slow-growing, so early and precise diagnosis is pivotal for disease therapy. Physical examination and particular biochemical markers tests are typically the first steps in the diagnostic process, while these biochemical indicators are typically present in a part of patients with functional tumors. Unspecific symptoms like bloating and weight loss are frequent in NET presentations, which can be challenging to identify or diagnose. It is also challenging to use conventional imaging techniques, such as computed tomography (CT), magnetic resonance imaging (MRI), and ultrasound (US), because some of the tumor lesions and metastases are small and can exist in different sites [3].

PET/CT is a technique that detects the lesions histomorphologic changes, and it can provide information about biomarkers and organizing morphology. The high sensitivity of PET/CT relies on specific biomarkers, metabolic pathways, and corresponding tracers. Somatostatin receptor (SSTR) is a specific biomarker in NETs for precise detection. High amounts of SSTR, especially subtypes 2 and 5, are expressed by well-differentiated NETs, which play a significant role in the diagnosis and therapy of NETs [4]. It had been proven feasible to use somatostatin analogues (SSAs), which detected the presence of SSTR, to image the distribution of NETs. Although [^{68}Ga]-labeled SSAs PET/CT are widely used in clinical NETs diagnosis, they have a limited capacity for lesions detection [5]. According to recent clinical studies, SSTR antagonists have better effects than agonists in lesion detection, tumor uptake, and tumor-to-background ratio (TBR) [6, 7]. In addition, the replacement of isotopes [^{68}Ga] with [^{64}Cu]/[^{18}F] leads to reduced cost, easy transportation, and improved spatial resolution, which facilitates small lesion detection [8]. [^{18}F]-FDG PET/CT is frequently used in undifferentiated or dedifferentiated Grade 3 (G3) NETs, as they are more heterogeneous and may not express SSTR. Some studies have focused on the C-X-C motif chemokine receptor 4 (CXCR4), which is overexpressed in aggressive and dedifferentiated NETs. [^{18}F]-MFBG and [^{18}F]-DOPA have a higher sensitivity for identifying non-metastatic pheochromocytoma and paraganglioma (PPGL) than other tracers. **Figures 1** and **2** exhibited the chemical structures of currently used and novel PET radiotracers for NET diagnosis.

Due to some novel radiotracers being investigated in recent years, this review aimed to provide an overview and comparison of NETs diagnostic ability with conventional imaging methods and PET/CT with various radiotracers. **Tables 1** and **2** showed the features of currently used and novel modalities for NETs.

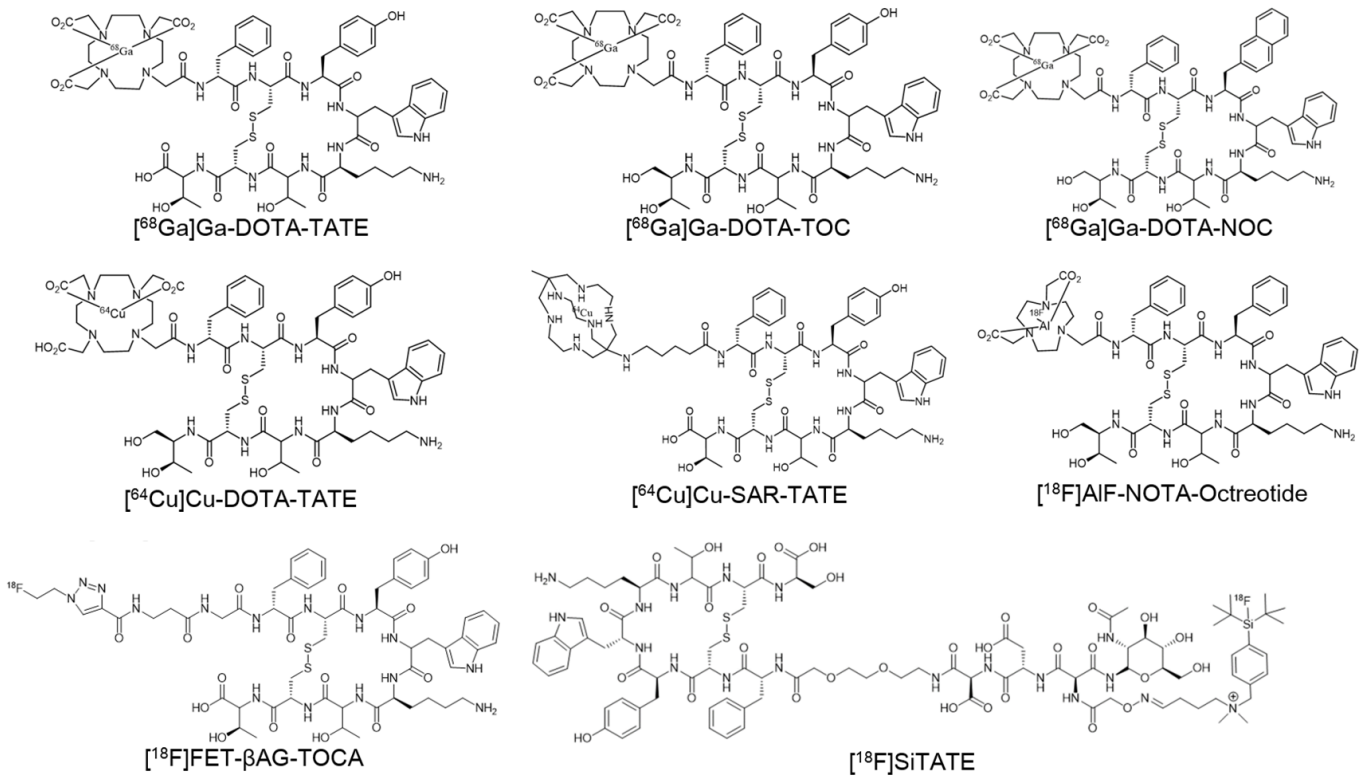

Figure 1. The structures of Somatostatin receptor agonists.

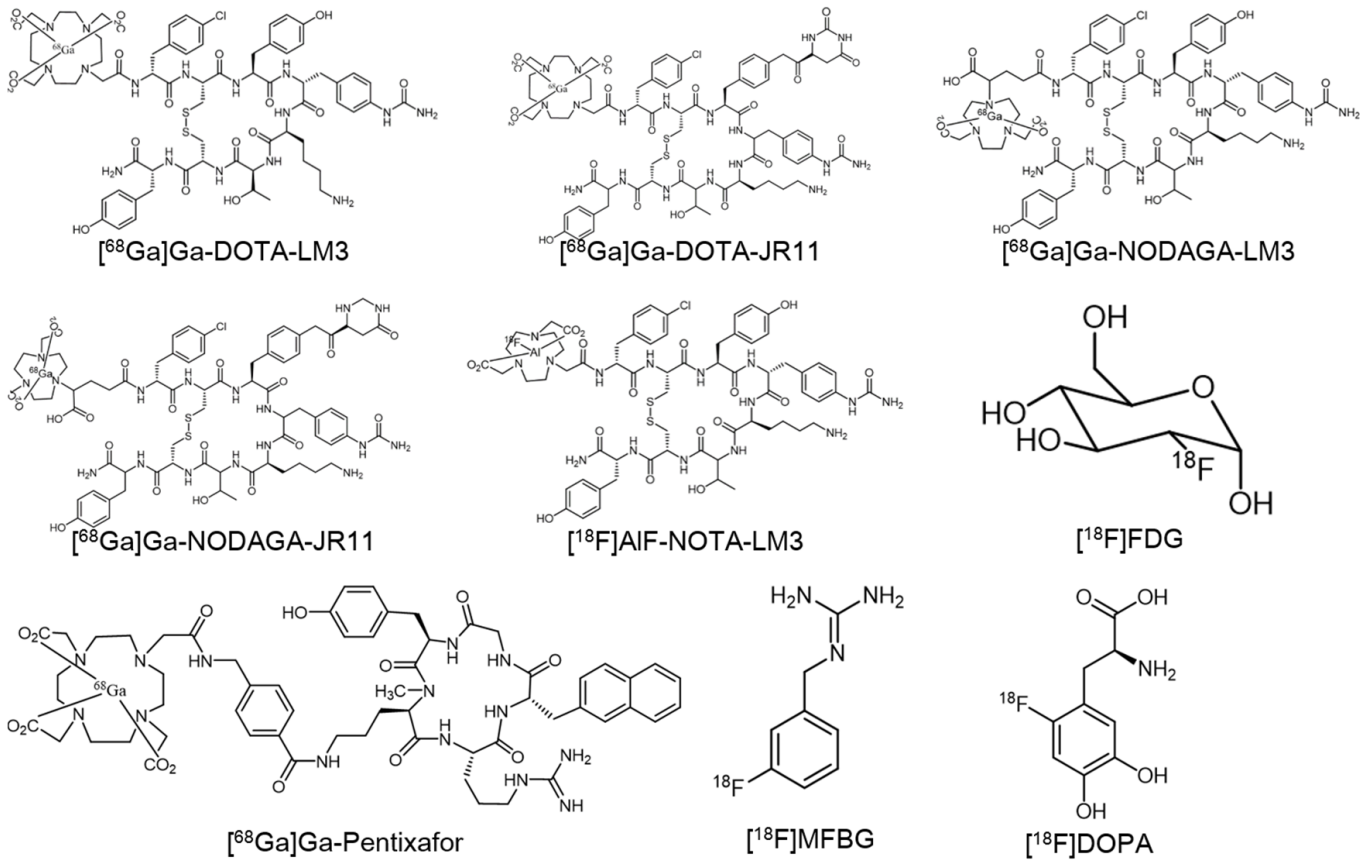

Figure 2. The structures of Somatostatin receptor antagonists and other novel radiotracers.

Table 1. Current used modalities for neuroendocrine tumors

Class	Radiotracer	Sensitive	Reference	Features	Limitation
Conventional imaging	CT	73%*	[11]	1. Initial imaging modality 2. Short acquisition time 3. Distinguish G1/G2 and G3 tumors	1. Low sensitivity to detect < 1 cm tumors and bone metastases 2. Variable specificity
	MRI	79%*	[20]	1. Complementary to CT 2. No radiation exposure 3. Detect PanNETs, hepatic metastases, and bone metastases	1. Relative contraindications 2. Less available than CT
SSTR agonist	[^{68}Ga]Ga-DOTA-TATE [^{68}Ga]Ga-DOTA-TOC [^{68}Ga]Ga-DOTA-NOC	92.3%* (G1) 90.2%* (G2) 57.8%* (G3)	[56] [56] [56]	1. Most widely used radiotracer for well-dfferentiated NETs 2. High sensitivity and specificity 3. Favorable biodistribution	1. High cost 2. High liver and spleen background 3. Short half-life
Glucose uptake	[^{18}F]FDG	37.8%* (G1) 55.4%* (G2) 71.2%* (G3)	[56] [56] [56]	1. Undifferentiated and dedifferentiated NETs 2. Heterogeneous disease 3. Prediction of prognosis	1. Not routinely used for NETs 2. Limited in well-differentiated NETs

Legends: NETs, neuroendocrine tumors; CT, Computed Tomography; NA, not applicable; MRI, Magnetic Resonance Imaging; G, grade; PanNETs, pancreatic neuroendocrine tumors; SSTR, somatostatin receptor; TBR, tumor-to-background ratio; *, depended on patient level.

Table 2. Emerging PET radiotracers for neuroendocrine tumors

Class	Radiotracer	Sensitive	Reference	Features
SSTR agonist	[^{64}Cu]Cu-DOTA-TATE	97%#	[52]	1. Long half-life, high TBR and low photon energy
	[^{64}Cu]Cu-SAR-TATE	NA	NA	2. Delayed imaging
	[^{18}F]AlF-NOTA-Octreotide	90.8%#	[73]	1. High TBR 2. Long half-life and increased spatial resolution
	[^{18}F]FET-βAG-TOCA	97.7%#	[65]	1. High TBR 2. Less synthesis time
	[^{18}F]SiTATE	NA	NA	1. Higher tumor-to-hepatic ratio and splenic ratio
SSTR antagonist	[^{68}Ga]Ga-DOTA-LM3	85.1%*	[39]	1. High TBR
	[^{68}Ga]Ga-DOTA-JR11	83.3%*	[39]	2. More receptor binding sites
	[^{68}Ga]Ga-NODAGA-LM3	92.5%*	[39]	3. Lower dissociation rate
	[^{68}Ga]Ga-NODAGA-JR11	96.5%*	[39]	
	[^{18}F]AlF-NOTA-LM3	90%*	[7]	
Chemokine receptor	[^{68}Ga]Ga-Pentixafor	80%* (G3)	[45]	1. Dedifferentiated and aggressive NET 2. Index of aggressiveness
Norepinephrine	[^{18}F]MFBG	98.5%#	[80]	1. Better than [^{123}I]MIBG 2. Neuroblastoma and PPGL
Amino acid analogue	[^{18}F]DOPA	95.7%*	[83]	1. Non-SDHx-associated PCC

Legends: TBR, tumor-to-background ratio; SSTR, somatostatin receptor; G, grade; PPGL, pheochromocytoma and paraganglioma; PCC, pheochromocytoma; NA, not applicable; *, depended on patient level; #, depended on lesion level.

Conventional imaging

As CT can be used for confirming the origin, staging, and monitoring treatment effects, it is the initial method to detect the lesions and determine the grade of NETs. Primary tumors and metastases typically showed hypervascularity and were detected in the early arterial phase [9]. The size, position, contrast with surrounding tissue, and image capture procedures all had an impact on sensitivity [9]. The diagnostic guideline for GEP NETs reported that the sensitivity of CT in the diagnosis of primary GEP NETs was about 73%, while rates varied greatly (63%-82%) [10]. A retrospective study on 69 pancreatic NETs (PanNETs) patients showed the ability of contrast-enhanced CT to precisely distinguish G1/G2 and G3 tumors [11]. PanNETs detection rates had been reported to be as high as 70%, especially the rates may be 80% to 100% when the primary tumors were larger than 2 cm [12]. Furthermore, Takumi et al. reported that there was a correlation between the CT features (M grade, tumor size, and tumor conspicuity) and the tumor grades of PanNETs [13]. CT also had high sensitivity and specificity in detecting hepatic metastases (sensitivity 82%, specificity 92%) and lymph node metastases (sensitivity 60%-70%, specificity 87%-100%) [10, 11]. In general, the sensitivity and specificity of CT to NET are lower than those of molecular imaging. The diagnostic effect is significantly impacted by the size of tumors, particularly when the diameter is smaller than 1 cm [14]. In addition, the average sensitivity to detect bone and soft tissue metastases outside of the liver ranges between 61% and 70% [15, 16]. Poorly distended intestine and the description of intestinal spasm as a pathology are the common errors leading to false positive diagnoses [17].

The signal intensity of typical NEN lesions is low in T1-weighted images and intermediate-to-high in T2-weighted images. Because of higher tissue resolution than CT and the use of several sequences, MRI is more beneficial to examine PanNETs, hepatic metastases, and bone metastases [18, 19]. Normal hepatocytes accumulate hepatocyte-specific MRI contrast media, including Gd-DTPA, to detect more metastases [14, 20]. Contrast administration improved the conventional T1- and T2-weighted images to obtain 79% sensitivity and almost 100% specificity in identifying PanNETs [20]. 75% of metastases were shown by a hypointense signal on T1-weighted images, and the majority of them were markedly enhanced in improved lesion detection and accuracy of lesion measurements after the administration of a contrast agent [10]. In research comparing hepatic metastases detecting methods, MRI had the highest sensitivity of 95.2%, while the sensitivity of CT was 78.5% [21]. MRI can also be helpful for patients who had iodinated contrast agent allergy [22]. When it comes to diagnosing extrapancreatic and extrahepatic lesions, MRI has a much lower sensitivity (68%-89%) [10]. However, the usual arterial phase enhancement and the hepatobiliary phase absence of enhancement following intravenous contrast injection were not unique to NETs [23]. Due to poor diagnostic performance, CT and MRI are not the optimal methods for diagnosing NETs.

[^{68}Ga]-labeled tracers

[^{68}Ga]Ga-labeled SSTR agonists

[^{68}Ga]Ga-DOTA-NOC is the pioneering compound for PET imaging, distinguished by its high affinity for the SSTR 2 and SSTR5 [24]. Since the first report of [^{68}Ga]Ga-DOTA-somatostatin analogs (SSAs) [25], SSTR agonists have been the most frequently used PET radiotracers for NETs detection at present. SSTR agonists PET/CT imagings have superiority over traditional SPECT imaging, especially for detecting small lesions, nodal, and bone metastases [26]. According to the current guideline for PET/CT imaging of NETs [27], [^{68}Ga]Ga-DOTA-SSAs PET/CT played a significant role in staging, re-staging following therapy, and prognostic evaluation. When it comes to the most type 2 SSTR expressed on NET cell surfaces, [^{68}Ga]Ga-DOTA-TATE has the highest affinity, which is a 10-fold binding tendency to [^{68}Ga]Ga-DOTA-NOC and [^{68}Ga]Ga-DOTA-TOC [28]. Despite having different SSTR-binding affinities, [^{68}Ga]Ga-DOTA-TOC, [^{68}Ga]Ga-DOTA-TATE, and [^{68}Ga]Ga-DOTA-NOC are regarded as clinically comparable with diagnostic accuracy [29, 30].

A recent meta-analysis [31] evaluated the impact of several radiotracers on diagnostic performance and clinical management in NETs or suspected NETs. SSTR PET/CT had over 90% sensitivity and specificity in well-differentiated NETs, and it can impact clinical management in over 40% of patients. Based on the degree of differentiation, the sensitivity of [^{68}Ga]Ga-DOTA-SSAs ranges from 92 to 100% for NET G1/G2, 67 to 92% for NET G3, and just 40 to 50% for NEC [32]. However, [^{68}Ga]Ga-DOTA-SSAs PET is not superb for its relatively short half-life (67.8 min) and high liver and spleen background. And the average positron energy of ^{68}Ga is relatively high (0.829 MeV), leading to a long average positron range (3.5 mm), which may compromise spatial resolution [33]. The above shortcomings limit the application of [^{68}Ga]Ga-DOTA-SSAs in diagnostic NETs, and new tracers need to be developed.

[^{68}Ga]Ga-labeled SSTR antagonists

In 2006, a study on cell uptake by Ginj et al. revealed that the quantity of binding sites on SSTR was many times higher for antagonists than for agonists [34]. Moreover, Ginj et al. reported that antagonists showed lower backgrounds and higher detection rates in mouse models [34]. Although [^{68}Ga]Ga-DOTA-TATE showed significantly higher type 2 SSTR affinity than antagonists [35], it did not lead to higher tumor uptake. SSTR antagonists, such as JR10, JR11, LM3, and LM4 series, were discovered and tested with various chelators and radionuclides. In a prospective phase I imaging study with 12 GEP NETs,

Nicolas et al. [36] reported the favorable safety, biodistribution, and imaging properties of [^{68}Ga]Ga-NODAGA-JR11. Subsequently, the phase II study [37] showed that [^{68}Ga]Ga-NODAGA-JR11 had much higher sensitivity (94% vs. 59%), reproducibility, and TBR (interquartile range 2.9-5.7 vs. 1.4-2.9, P = 0.004) than [^{68}Ga]Ga-DOTA-TOC. LM4 was a new SSTR2 antagonist derived from LM3. It was labeled with [^{68}Ga] utilizing DATA^{5m} and showed higher SSTR2 affinity than LM3 [38]. In a recently published prospective study, [^{68}Ga]Ga-DATA^{5m}-LM4 showed higher lesion-based sensitivity (94.28% vs. 83.46%, P < 0.001) and TBR than [^{68}Ga]Ga-DOTA-TOC [39]. The superiority of sensitivity was reflected in accurately identifying liver (292 vs. 253) and bone (45 vs. 34) metastases.

In a recently published large retrospective study evaluated by Liu et al., a comparative [^{68}Ga]Ga-DOTA-TATE PET/CT was performed on 181 of the 549 NETs who received a diagnosis based on the four antagonists ([^{68}Ga]Ga-NODAGA-LM3, [^{68}Ga]Ga-NODAGA-JR11, [^{68}Ga]Ga-DOTA-LM3, [^{68}Ga]Ga-DOTA-JR11) [40]. Compared to [^{68}Ga]Ga-DOTA-TATE (86.7%), [^{68}Ga]Ga-NODAGA-LM3 (92.5%) and [^{68}Ga]Ga-NODAGA-JR11 (96.5%) showed significantly superior accuracy, while [^{68}Ga]Ga-DOTA-LM3 (85.1%) and [^{68}Ga]Ga-DOTA-JR11 (83.3%) showed lower diagnostic efficacy. In the hottest lesions (maximum standardized uptake lesions), [^{68}Ga]Ga-NODAGA-LM3 showed higher tumor uptake than [^{68}Ga]Ga-DOTA-TATE (SUV_{max}, 40.0 ± 22.8 vs. 57.4 ± 38.5, P < 0.001), whereas the other antagonists were no better than [^{68}Ga]Ga-DOTA-TATE. Liver lesions TBR of SSTR antagonists was significantly higher than [^{68}Ga]Ga-DOTA-TATE (12.1 ± 10.8 vs. 5.2 ± 4.5, P < 0.001) [40]. [^{68}Ga]Ga-NODAGA-LM3 had superiority for detecting more liver metastases than [^{68}Ga]Ga-DOTA-TATE (**Figure 4E**) [41]. In a head-to-head comparison of [^{68}Ga]Ga-DOTA-TATE and [^{68}Ga]Ga-DOTA-JR11, Zhu et al. reported that the reduced osseous lesion detection rate of [^{68}Ga]Ga-DOTA-JR11 indicated lower bone marrow radioactivity uptake (no statistically significant) [42]. In conclusion, [^{68}Ga]Ga-NODAGA-LM3 showed the best imaging performance among the [^{68}Ga]-labeled SSTR antagonists. As the antagonist shows excellent diagnostic efficacy, it is necessary to combine the antagonist PET/CT with [^{18}F]-FDG PET/CT to detect lesions.

[^{68}Ga]Ga-Pentixafor

G3 NETs typically failed to respond well to treatments with SSTR analogs because these receptors were not expressed in enough quantity [43]. When it comes to tumors that did not express SSTR well, [^{18}F]-FDG was typically the preferred PET tracer. According to previous studies, CXCR4 was linked to the occurrence, progression, invasion, and metastasis of several kinds of malignant tumors [44, 45]. Kaemmerer et al. reported that the aggressive and dedifferentiated NETs also exhibited overexpression of CXCR4 [43]. In a triple tracers ([^{68}Ga]Ga-Pentixafor, [^{18}F]-FDG, and [^{68}Ga]Ga-DOTA-TOC) comparative research on 12 patients with histologically proven GEP-NETs, Werner et al. showed that [^{68}Ga]Ga-Pentixafor (radiotracer targeting CXCR4) PET exhibited positive tumor lesions in 80% of G3 patients, but it was negative in all G1 NETs [46]. **Figure 4D** demonstrated hepatic metastatics with loss of SSTR and up-regulation of CXCR4 expression. Weich et al. [47] evaluated the comparison of [^{68}Ga]Ga-Pentixafor and [^{18}F]-FDG PET/CT in 11 patients with poorly differentiated NECs. [^{18}F]-FDG showed significantly higher superiority in detecting tumor lesions (102 vs. 42, P < 0.001) and tumor uptake (SUV_{max}: 12.8 ± 9.8 vs. 5.2 ± 3.7, P < 0.001). Weich et al. recently found that [^{68}Ga]Ga-Pentixafor missed 13 patients with digestive system tumors, resulting in 10 patients receiving improper downstaging and treatment [48]. Michalski et al. discovered a significant correlation between tumor volume (TV) and total-lesion uptake (TLU) for overall survival (OS) (TV: hazard ratio (HR) 1.007, P = 0.0309; TLU: HR = 1.002, P = 0.0350) and rPFS (TV: HR = 1.010; P = 0.0275; TLU: HR = 1.002, P = 0.0329), respectively [49]. Pang et al. reported that there were notable differences between NET G3 and NEC in tumor site, CXCR4 expression, and Ki-67 index [50]. However, according to the Kaplan-Meier curves, patients with high and low CXCR4 expression had no significant differences in OS in either GEP-NEN G3 or NEC (P = 0.920 and P = 0.842, respectively) [50]. Therefore, CXCR4 is a potential target for NETs, but [^{68}Ga]Ga-Pentixafor has not shown better clinical application.

[^{64}Cu]-labeled tracers

[^{64}Cu]Cu-DOTA-TATE

[^{64}Cu] had a longer half-life (12.7 h) than [^{68}Ga], which can lead to higher TBR on delayed imaging [51]. It also had a lower positron energy (0.278 MeV) and shorter positron range (0.8 mm) than [^{68}Ga]. In the first-in-humans study of [^{64}Cu]Cu-DOTA-TATE compared with conventional scintigraphy, Pfeifer et al. discovered that [^{64}Cu]Cu-DOTA-TATE detected additional lesions in 6 of 14 patients (43%) and had excellent imaging quality [52]. The advantages of [^{64}Cu] contributed to better imaging characteristics, particularly on 3-24 hours post injection delayed imaging of 112 patients with proven NETs [53]. In a prospective study on 59 NET patients, [^{64}Cu]Cu-DOTA-TATE detected more lesions (675 vs. 659) than [^{68}Ga]Ga-DOTA-TOC with no significant difference [54]. All organs except the spleen had lower physiologic background uptake of the tracers for [^{68}Ga]Ga-DOTA-TOC than for [^{64}Cu]Cu-DOTA-TATE (**Figure 3C**). In intestinal, pancreatic, liver, lymph nodes, and carcinomatosis lesions, SUV_{max} was significantly higher for [^{64}Cu]Cu-DOTA-TATE than for [^{68}Ga]Ga-DOTA-TOC. Moreover, equivalent detection of lesions for 1 h (821 lesions) and 3 h (818 lesions) imaging was shown by Loft et al. in 35 NET patients, indicating that the imaging window of 200 MBq [^{64}Cu]Cu-DOTA-TATE PET/CT can be expanded from 1 h to 1-3 h [55]. Subsequently, Loft et al. showed that the [^{64}Cu]Cu-DOTA-TATE activity dose can be

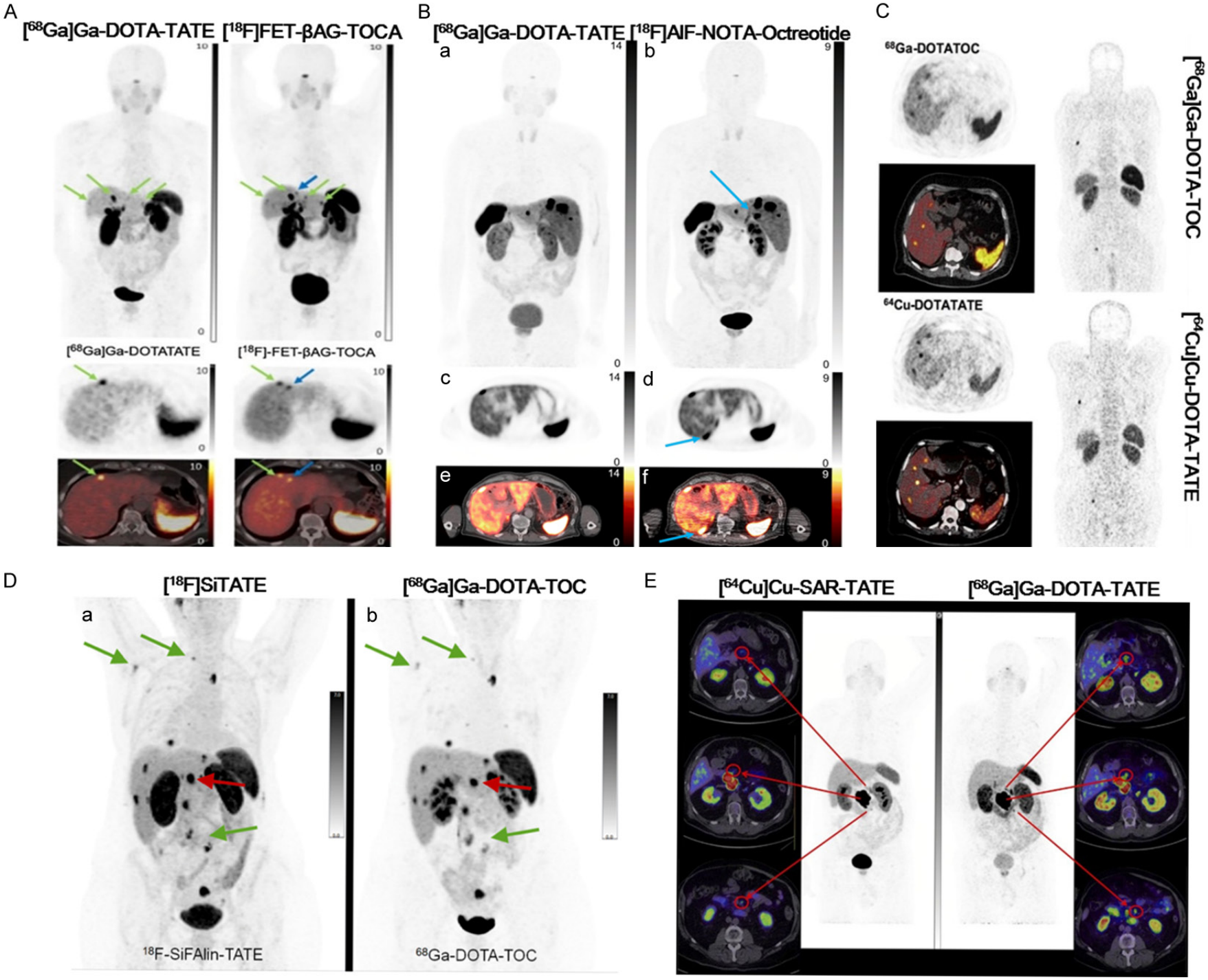
A
[68Ga]Ga-DOTA-TATE
[18F]FET-βAG-TOCA
[68Ga]Ga-DOTATATE
[18F]-FET-βAG-TOCA
B
[68Ga]Ga-DOTA-TATE
[18F]AlF-NOTA-Octreotide
a
b
c
d
e
f
C
68Ga-DOTATOC
64Cu-DOTATATE
[68Ga]Ga-DOTA-TOC
[64Cu]Cu-DOTA-TATE
D
[18F]SiTATE
[68Ga]Ga-DOTA-TOC
a
b
18F-SiFAlin-TATE
68Ga-DOTA-TOC
E
[64Cu]Cu-SAR-TATE
[68Ga]Ga-DOTA-TATE

Figure 3. The imaging comparison of novel SSTR agonists with [^{68}Ga]Ga-DOTA SSAs in patients. A: [^{18}F]FET-βAG-TOCA imaging performed more visibly than [^{68}Ga]Ga-DOTA-TATE in metastatic ileal NEN with liver metastases (green arrows) and detected an additional lesion (blue arrow). B: [^{18}F]AlF-NOTA-Octreotide imaging detected an additional liver lesion that was missed by the [^{68}Ga]Ga-DOTA-TATE scan (blue arrow). C: Foci were more distinct with [^{64}Cu]Cu-DOTA-TATE than with [^{68}Ga]Ga-DOTA-TOC. D: The preferable image quality of [^{18}F]SiTATE was apparent in smaller tumor lesions with more uptake than [^{68}Ga]Ga-DOTA-TOC (green arrows). Most lesions showed high uptake in both scans (red arrow). E: [^{64}Cu]Cu-SAR-TATE imaging at 4 h better defined regional nodal disease than [^{68}Ga]Ga-DOTA-TATE at 1 h in patient with large pancreatic primary tumor but slightly greater small-bowel activity.

reduced from 191 MBq to 142 MBq without decreasing image quality or lesion detection ability [56].

[^{64}Cu]Cu-SAR-TATE

Compared to DOTA complexes, SAR may offer more stable binding with copper and may offer prolonged radiotracer retention in lesions [57]. [^{64}Cu]Cu-SAR-TATE is a novel SSTR agonist PET agent that has been developed and evaluated in preclinical settings. In a first-in-humans trial by Hicks et al. on 10 NET patients with [^{68}Ga]Ga-DOTA-TATE PET/CT positive imaging, [^{64}Cu]Cu-SAR-TATE was well tolerated throughout the study [58]. Serial [^{64}Cu]Cu-SAR-TATE PET/CT images timed at 30 min, 1 h, 4 h, and 24 h were taken after the radiotracer injection to evaluate the high late retention and clearance from the liver [58]. For the majority of patients, the imaging quality obtained 1 h after [^{64}Cu]Cu-SAR-TATE injection was equivalent to [^{68}Ga]Ga-DOTA-TATE [58]. Regional nodal disease was better defined by high lesion contrast on [^{64}Cu]Cu-SAR-TATE images taken at 4 hours than by [^{68}Ga]Ga-DOTATATE images taken at 1 hour (**Figure 3E**). It was interesting to see the progressive increase of TBR in [^{64}Cu]Cu-SAR-TATE scans from 4 to 24 hours. Therefore, delayed imaging can enable more accurate lesion diagnosis and enhanced sensitivity at the liver level. It had also been demonstrated by Laffon et al. that [^{64}Cu]Cu-SAR-TATE PET/CT performed well in the diagnosis of patients with neuroblastoma, but it needs further clinical investigation [59]. [^{64}Cu] has advantages in half-life and spatial resolution, but there is no significant difference between [^{64}Cu]Cu-SSAs and [^{68}Ga]Ga-DOTA-SSAs in the detection of lesions.

[^{18}F]-labeled tracers

[^{18}F]-FDG

Because G3 NETs typically have low SSTR expression, [^{18}F]-FDG PET/CT can show better sensitivity and prognostic performance [60]. In a recently published meta-analysis comparing [^{68}Ga]Ga-DOTA-SSAs and [^{18}F]-FDG PET/CT on 3401 NET patients, Liu et al. showed that [^{68}Ga]Ga-DOTA-SSAs PET/CT had considerably higher sensitivity and diagnostic utility in G1 (92.3% vs. 37.8%) and G2 (90.2% vs. 55.4%) NETs; [^{18}F]-FDG PET/CT had better sensitivity and utility in G3 NETs (71.2% vs. 57.8%) [57]. According to a comprehensive meta-analysis of 23 original articles, [^{18}F]-FDG PET/CT offered a greater role in risk stratification for G3 NETs than G1 and G2 NETs [61]. High FDG uptake in NETs was associated with a 2.84-fold higher risk of disease progression and recurrence, as well as a 3.5-fold increased risk of death [61].

Due to the coexistence of various grade lesions and the intra-tumor and inter-tumor heterogeneity in a patient, combining [^{68}Ga]Ga-DOTA-SSAs and [^{18}F]-FDG PET/CT can show more predictive information for treatment outcome and monitoring [62]. The NET-PET score developed by Chan et al. [62] indicated the connection between glucose metabolism and SSTR expression to standardize reporting of concordance between the two scans. According to a multicenter validation of the NETPET score, Chan et al. assessed the total discordant volume (TDV) in 44 patients with proven GEP-NETs [63]. TDV was calculated by adding the volumes of mismatched lesions between ^{18}F-FDG and [^{68}Ga]Ga-DOTA-TATE PET/CT. Compared to the high TDV group, the overall survival of the low TDV group was longer (median volume, 43.7 cm^3; survival time, 23.8 mo vs. 9.4 mo; P = 0.022), which may be relative to that function failure due to more lesions [63]. [^{18}F]FDG PET/CT is highly effective in detecting high-grade tumors and offers valuable insights into tumor classification and prognosis.

[^{18}F]FET-βAG-TOCA

Dubash et al. firstly reported that the favorable safety profile, coupled with its robust imaging and dosimetric characteristics, positions [^{18}F]FET-βAG-TOCA as a promising tracer for the staging and management of NETs [64]. [^{18}F]FET-βAG-TOCA was an SSTR-2 targeting tracer and had a quicker synthesis time than other [^{18}F]-octreotate analogs [65]. In a first-in-human study on 9 NET patients, Dubash et al. demonstrated the safety and well-tolerance of [^{18}F]FET-βAG-TOCA [64]. The gallbladder had the maximum absorbed dosage, followed by the spleen, stomach wall, liver, kidneys, and bladder. [^{18}F]FET-βAG-TOCA had a high TBR and tumor uptake in every organ, which were similar to [^{68}Ga]Ga-DOTA-SSAs [64]. In a larger study on 45 patients, Dubash et al. confirmed the non-inferiority of [^{18}F]FET-βAG-TOCA to [^{68}Ga]Ga-DOTA-TATE for NETs in tumor SUV_{max} (no significant difference) [66]. In a NET patient with liver metastases, [^{18}F]FET-βAG-TOCA imaging was more visible and detected an additional lesion (**Figure 3A**). In 285 lesions found by two tracers, [^{18}F]FET-βAG-TOCA detected more tumor lesions (278 vs. 272) than [^{68}Ga]Ga-DOTA-TATE PET/CT. Because the liver background uptake of [^{18}F]FET-βAG-TOCA was much lower, it had significantly higher hepatic TBR than [^{68}Ga]Ga-DOTA-TATE (2.52 ± 1.88 vs. 3.50 ± 2.35; P < 0.001). Given the encouraging outcomes of [^{18}F]FET-βAG-TOCA for lesion

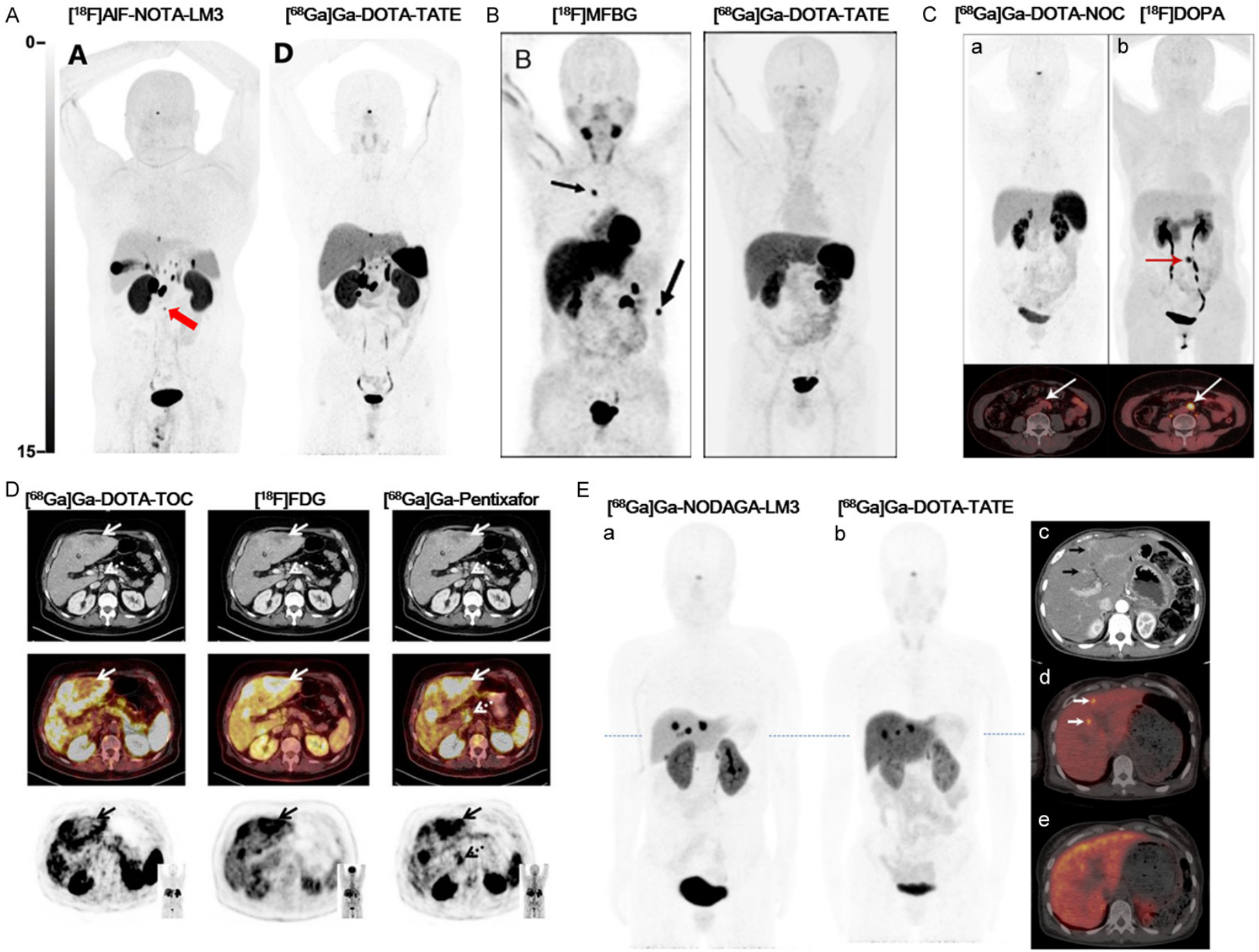
A
[18F]AlF-NOTA-LM3
[68Ga]Ga-DOTA-TATE
0
15
A
D
B
[18F]MFBG
[68Ga]Ga-DOTA-TATE
B
C
[68Ga]Ga-DOTA-NOC
[18F]DOPA
a
b
D
[68Ga]Ga-DOTA-TOC
[18F]FDG
[68Ga]Ga-Pentixafor
E
[68Ga]Ga-NODAGA-LM3
[68Ga]Ga-DOTA-TATE
a
b
c
d
e

Figure 4. The imaging comparison of other radiotracers with conventional imaging in patients. A: [^{18}F]AlF-NOTA-LM3 (red arrows) revealed a positive para-aortic lymph node lesion that was missed by [^{68}Ga]Ga-DOTATATE. B: [^{18}F]MFBG PET/CT showed metastases in the fourth thoracic vertebra (small arrow) and the left 10th rib (larger arrow), which were all negative on [^{68}Ga]Ga-DOTATATE image. C: Tumors (arrows) exhibited intense [^{18}F]DOPA avidity but were negative on [^{68}Ga]Ga-DOTA-NOC PET/CT. D: Hypermetabolic hepatic metastases demonstrated loss of SSTR and up-regulation of CXCR4 expression in G3 NETs (solid arrows, corresponding SUVmax: 10.3 for [^{68}Ga]Ga-Pentixafor, and 3.8 for [^{68}Ga]Ga-DOTA-TOC). [^{68}Ga]Ga-Pentixafor provided additional information on disease extent by detecting a coeliacal lymph node suspicious for metastatic disease (dotted arrows). E: [^{68}Ga]Ga-NODAGA-LM3 scan demonstrated two sub-centimeter lesions (white arrows) at the level of blue dash line and were further confirmed on contrast-enhanced CT (black arrows) performed within a month. [^{68}Ga]Ga-DOTA-TATE failed to detect these two lesions.

detection, it may be a possible substitute for [^{68}Ga]Ga-DOTA-SSAs.

[^{18}F]SiTATE

[^{18}F]SiTATE can be produced with good manufacturing techniques and has shown strong selectivity for SSTR2 [67]. A patient with metastatic NETs underwent the first-in-human [^{18}F]SiTATE PET/CT [68]. [^{18}F]SiTATE revealed bone and cardiac metastases uptake similar to [^{68}Ga]Ga-DOTA-TATE [68]. In a retrospective study on 13 NET patients, Ilhan et al. compared the tumor uptake, biodistribution, and image quality of [^{18}F]SiTATE and [^{68}Ga]Ga-DOTA-TOC [69]. The kidney physiologic uptake (20.7 ± 6.7 vs. 14.4 ± 4.1; P < 0.02) of ^{18}F-SiTATE was substantially higher than that of [^{68}Ga]Ga-DOTA-TOC [69]. The biodistribution was similar to [^{68}Ga]Ga-DOTA-TATE, with the largest radiotracer uptake in the bladder and spleen, followed by the kidneys and adrenal glands [69]. With focally increased uptake, the superior image quality of [^{18}F]SiTATE was particularly obvious in smaller tumor lesions (**Figure 3D**). Additionally, tumor lesions in common metastatic sites showed a much increased tumor uptake, except lung lesions. Beyer et al. reported that 120 min after injection was the ideal imaging time for balancing TBR and image quality [70]. Eschbach et al. examined the impact of previous treatment with long-acting SSAs before [^{18}F]SiTATE on tumor uptake and physiologic uptake [71]. This condition was associated with a considerably decreased [^{18}F]SiTATE physiologic uptake in the liver and spleen [71]. Because there was no significant decrease in TBR, it was recommended not to stop using SSA treatment before [^{18}F]SiTATE PET/CT. [^{18}F]SiTATE has important value in the diagnosis, staging, treatment guidance and prognosis assessment of NETs.

[^{18}F]AlF-NOTA-Octreotide

[^{18}F]AlF-NOTA-Octreotide, a new SSTR agonist tagged with fluorine, had been developed [72]. In a first-in-humans study on 22 proven NET patients, Long et al. compared [^{18}F]AlF-NOTA-Octreotide PET/CT and [^{18}F]-FDG PET/CT [73]. The spleen, kidneys, and bladder exhibited high physiologic [^{18}F]AlF-NOTA-Octreotide uptake [73]. **Figure 3B** showed that [^{18}F]AlF-NOTA-Octreotide detected an additional liver lesion. [^{18}F]AlF-NOTA-Octreotide was more sensitive than [^{18}F]-FDG in lesion detection (624 vs. 390). They reported that G2 NETs had higher [^{18}F]AlF-NOTA-Octreotide uptake (median SUV_{max}, 4.3 vs. 45.6; P < 0.015) than [^{18}F]-FDG, while higher [^{18}F]-FDG uptake was shown in poorly differentiated NETs (median SUV_{max}, 7.6 vs. 12.6; P = 0.594) [73]. Pauwels et al. reported that out of 4709 tumor lesions total, [^{68}Ga]Ga-DOTA-TATE/NOC found 3454 lesions, and [^{18}F]AlF-NOTA-Octreotide detected 4278 lesions in a prospective multicenter trial on 75 patients with histologically confirmed NET [74]. [^{18}F]AlF-NOTA-Octreotide showed higher detection ratios (DR) for most organs than [^{68}Ga]Ga-DOTA-SSAs, excepting bone lesions (mean different DR, -2.8%; 95% CI, -17.8 to 12.2). The favorable diagnostic accuracy of [^{18}F]AlF-NOTA-Octreotide was confirmed in another trial including 162 NET patients by Hou et al. [75]. It was interesting to note that benign lesions had different conditions of [^{18}F]AlF-NOTA-Octreotide uptake, which was consistent with the uptake patterns of [^{68}Ga]Ga-DOTA-SSAs [75, 76]. Although [^{18}F]AlF-NOTA-Octreotide will have deficiencies in cases with metastases of multiple bone lesions, it is a promising tracer for detecting NETs.

[^{18}F]-labeled SSTR antagonists

Xie et al. synthesized the first [^{18}F]-labeled SSTR antagonist and used tumor-bearing mice for preclinical research [77]. Due to the low background tracer uptake of [^{18}F]AlF-NOTA-JR11, it detected more lesions than [^{68}Ga]Ga-DOTA-TATE in the stomach, liver, and pancreas. Ahenkorah developed an automated method to radiosynthesize [^{18}F]AlF-NOTA-JR11 and showed similar images to [^{18}F]AlF-NOTA-Octreotide [78]. In a prospective head-to-head study comparing [^{18}F]AlF-NOTA-LM3 with [^{68}Ga]Ga-DOTA-TATE, Liu et al. reported favorable safety, dosimetry features, and biodistribution of [^{18}F]AlF-NOTA-LM3 [7]. When compared to [^{68}Ga]Ga-DOTA-TATE, [^{18}F]AlF-NOTA-LM3 can detect more lymph node lesions (22 vs. 30, P = 0.011) and liver lesions (291 vs. 457, P = 0.006). [^{18}F]AlF-NOTA-LM3 proved especially useful in detecting tiny lesions that [^{68}Ga]Ga-DOTA-TATE would overlook (**Figure 4A**). Moreover, [^{18}F]AlF-NOTA-LM3 was the first SSA that showed favorable performance in detecting lymph node lesions. [^{18}F]-labeled SSTR antagonists hold significant potential for the diagnosis of NETs, but the current research remains limited.

[^{18}F]MFBG

Pheochromocytoma (PCC) and paraganglioma (PGL), collectively known as PPGL, are uncommon NETs. [^{18}F]MFBG was a fluorinated analogue of [^{123}I]MIBG and was

accumulated by the equivalent norepinephrine transporter uptake mechanism as [^{123}I]MIBG. Although [^{123}I]MIBG showed high sensitivity for detecting PPGL, [^{123}I]MIBG imaging had low quantitative accuracy, lengthy scan acquisition times, and poor imaging quality [79, 80]. In a first-in-human prospective study on 10 patients with confirmed neuroblastoma or PPGL [79], Tastar et al. demonstrated that [^{18}F]MFBG was favorably tolerated and had an analogous biodistribution to [^{123}I]MIBG. Because 1-2 h after ^{18}F-MFBG PET/CT injection displayed the highest TBR (1.35-36.2) for soft tissue and bone lesions, it provided favorable imaging quality and lesion detection (63 vs. 122). In a prospective trial on 28 patients with 686 foci of metastatic PPGL lesions by [^{18}F]MFBG and [^{68}Ga]Ga-DOTA-TATE, Wang et al. showed that [^{18}F]MFBG detected more abnormal foci than [^{68}Ga]Ga-DOTA-TATE (33 vs. 16) [81]. In contrast to the [^{68}Ga]Ga-DOTATATE images, [^{18}F]MFBG PET/CT revealed additional metastases in the left 10th rib and the fourth thoracic vertebra (**Figure 4B**). [^{18}F]MFBG has demonstrated significant potential in the diagnosis of PPGLs, proving to be more effective than [^{123}I]MIBG and [^{68}Ga]Ga-DOTATATE.

[^{18}F]DOPA

[^{18}F]DOPA is an amino acid radiotracer that has a high uptake in tumors and a low uptake in the right brain [82]. Because of enhanced uptake, [^{18}F]DOPA can be accumulated specifically in PPGLs. According to a review on personalized management of PPGLs, [^{18}F]DOPA PET/CT was a preferred functional imaging method for cluster 1B and 2 tumors [83]. In a recent prospective study on 32 patients, [^{18}F]DOPA had noninferior sensitivity (95.7% vs. 91.3%) and equivalent specificity to [^{123}I]MIBG SPECT/CT (88.9% vs. 88.9%) in the patient-level diagnosis of PPGLs [84]. However, [^{18}F]DOPA PET/CT showed better interreader agreement (κ = 0.94 vs. 0.85) and sensitivity (86.2% vs. 65.5%, P = 0.031) to assess metastases and recurrence. In a study on 85 patients with histopathologically confirmed PPGLs, He et al. showed that [^{18}F]DOPA and [^{68}Ga]Ga-DOTA-NOC can be complementary methods to diagnose PPGL in certain clinical conditions [85]. [^{68}Ga]Ga-DOTA-NOC PET/CT could detect sympathetic PGL metastases and SDHx-related PPGLs for superior diagnostic performance and detection rate. However, ^{18}F-DOPA is the best radiotracer for assessing non-SDHx-associated PCC, particularly primary lesions and recurrence [85]. Comparison of the PET/CT imaging of the nonmetastatic case with positive results only on [^{18}F]DOPA PET/CT was shown in **Figure 4C**. As current studies on [^{18}F]MBFG PET/CT and [^{18}F]DOPA PET/CT in PPGLs were limited, further research is necessary to compare the excellent diagnostic protocols.

Conclusion

Novel radiotracers for nuclear medicine hold the potential to improve NET detection and more accurately reflect the molecular features of tumors, offering understanding of both intra-tumor and inter-tumor heterogeneity. [^{18}F]-labeled SSTR agonists ([^{18}F]AlF-NOTA-Octreotide, [^{18}F]FET-βAG-TOCA, and [^{18}F]SiTATE) and antagonists ([^{18}F]AlF-NOTA-LM3 and [^{68}Ga]Ga-NODAGA-LM3) are promising tracers to substitute [^{68}Ga]Ga-DOTA-SSAs in diagnosing G1 and G2 NETs. Clinical studies on a range of tracers typically showed that they performed better than [^{68}Ga]Ga-DOTA-SSAs in terms of biodistribution, TBR, and lesion detection. The dual-tracer strategy ([^{68}Ga]Ga-SSAs + [^{18}F]FDG) has demonstrated remarkable performance in detecting high-grade (G3) NETs and SSTR-negative NETs. The validation and generalization of NETPET scores in multicenter studies is crucial for providing clinicians with a standardized assessment tool to optimize treatment and enhance patient survival. Although many novel tracers have excellent diagnostic performance, the use of novel tracers should take clinical translation challenges (e.g., cost, accessibility) into account. More multicenter clinical studies and head-to-head comparisons with larger patient populations and longer follow-ups to demonstrate the safety, diagnostic accuracy, sensitivity, and specificity profiles of new tracers are warranted.

Acknowledgements

This study was funded in part by the National Natural Science Foundation of China (82171982); the Natural Science Foundation of Fujian Province (2023J06031); and the Tianjin Key Medical Discipline (Specialty) Construction Project (TJYXZDXK-001A).

Written informed consent was not required for this study because this is a review.

Disclosure of conflict of interest

None.

Address correspondence to: Drs. Qiusong Chen and Shaobo Yao, Department of PET/CT Diagnostic, Tianjin Key Lab of Functional Imaging and Tianjin Institute of Radiology, Tianjin Medical University General Hospital, No. 154 Anshan Road, Heping District, Tianjin 300052, China. Tel: +86-022-60362190; E-mail: qs_c8@hotmail.com (QSC); yaoshaobo008@163.com (SBY)

References

[1] Hauso O, Gustafsson BI, Kidd M, Waldum HL, Drozdov I, Chan AK and Modlin IM. Neuroendocrine tumor epidemiology: contrasting Norway and North America. Cancer 2008; 113: 2655-2664.

[2] Das S and Dasari A. Epidemiology, incidence, and prevalence of neuroendocrine neoplasms: are there global differences? Curr Oncol Rep 2021; 23: 43.

[3] Ebner R, Sheikh GT, Brendel M, Ricke J and Cyran CC. ESR Essentials: role of PET/CT in neuroendocrine tumors-practice recommendations by the European Society for Hybrid,

Molecular and Translational Imaging. Eur Radiol 2024; [Epub ahead of print].
[4] Strosberg JR, Al-Toubah T, El-Haddad G, Reidy Lagunes D and Bodei L. Sequencing of somatostatin-receptor-based therapies in neuroendocrine tumor patients. J Nucl Med 2024; 65: 340-348.
[5] Pavel M, Öberg K, Falconi M, Krenning EP, Sundin A, Perren A and Berruti A. Gastroenteropancreatic neuroendocrine neoplasms: ESMO clinical practice guidelines for diagnosis, treatment and follow-up. Ann Oncol 2020; 31: 844-860.
[6] Lin Z, Zhu W, Zhang J, Miao W, Yao S and Huo L. Head-to-head comparison of (68)Ga-NODAGA-JR11 and (68)Ga-DOTATATE PET/CT in patients with metastatic, well-differentiated neuroendocrine tumors: interim analysis of a prospective bicenter study. J Nucl Med 2023; 64: 1406-1411.
[7] Liu M, Ren C, Zhang H, Zhang Y, Huang Z, Jia R, Cheng Y, Bai C, Xu Q, Zhu W and Huo L. Evaluation of the safety, biodistribution, dosimetry of [(18)F]AlF-NOTA-LM3 and head-to-head comparison with [(68)Ga]Ga-DOTATATE in patients with well-differentiated neuroendocrine tumors: an interim analysis of a prospective trial. Eur J Nucl Med Mol Imaging 2024; 51: 3719-3730.
[8] Leupe H, Ahenkorah S, Dekervel J, Unterrainer M, Van Cutsem E, Verslype C, Cleeren F and Deroose CM. (18)F-labeled somatostatin analogs as PET tracers for the somatostatin receptor: ready for clinical use. J Nucl Med 2023; 64: 835-841.
[9] Sahani DV, Bonaffini PA, Fernández-Del Castillo C and Blake MA. Gastroenteropancreatic neuroendocrine tumors: role of imaging in diagnosis and management. Radiology 2013; 266: 38-61.
[10] Kos-Kudła B, Foltyn W, Malczewska A, Bednarczuk T, Bolanowski M, Borowska M, Chmielik E, Ćwikła JB, Gisterek I, Handkiewicz-Junak D, Hubalewska-Dydejczyk A, Jarząb B, Jarząb M, Junik R, Kajdaniuk D, Kamiński G, Kolasińska-Ćwikła A, Kowalska A, Królicki L, Krzakowski M, Kunikowska J, Kuśnierz K, Lewiński A, Liszka Ł, Londzin-Olesik M, Marek B, Nasierowska-Guttmejer A, Nowakowska-Duława E, Pavel ME, Pilch-Kowalczyk J, Reguła J, Rosiek V, Ruchała M, Rydzewska G, Siemińska L, Sowa-Staszczak A, Starzyńska T, Stojčev Z, Strzelczyk J, Studniarek M, Syrenicz A, Szczepkowski M, Wachuła E, Zajęcki W, Zemczak A, Zgliczyński W and Zieniewicz K. Update of the diagnostic and therapeutic guidelines for gastro-entero-pancreatic neuroendocrine neoplasms (recommended by the Polish network of neuroendocrine tumours) [Aktualizacja zaleceń ogólnych dotyczących postępowania diagnostyczno-terapeutycznego w nowotworach neuroendokrynnych układu pokarmowego (rekomendowane przez Polską Sieć Guzów Neuroendokrynnych)]. Endokrynol Pol 2022; 73: 387-454.
[11] Park HJ, Kim HJ, Kim KW, Kim SY, Choi SH, You MW, Hwang HS and Hong SM. Comparison between neuroendocrine carcinomas and well-differentiated neuroendocrine tumors of the pancreas using dynamic enhanced CT. Eur Radiol 2020; 30: 4772-4782.
[12] Diebold AE, Boudreaux JP, Wang YZ, Anthony LB, Uhlhorn AP, Ryan P, Mamikunian P, Mamikunian G and Woltering EA. Neurokinin A levels predict survival in patients with stage IV well differentiated small bowel neuroendocrine neoplasms. Surgery 2012; 152: 1172-1176.
[13] Takumi K, Fukukura Y, Higashi M, Ideue J, Umanodan T, Hakamada H, Kanetsuki I and Yoshiura T. Pancreatic neuroendocrine tumors: correlation between the contrast-enhanced computed tomography features and the pathological tumor grade. Eur J Radiol 2015; 84: 1436-1443.
[14] Hofland J, Kaltsas G and de Herder WW. Advances in the diagnosis and management of well-differentiated neuroendocrine neoplasms. Endocr Rev 2020; 41: 371-403.
[15] Pilleul F, Penigaud M, Milot L, Saurin JC, Chayvialle JA and Valette PJ. Possible small-bowel neoplasms: contrast-enhanced and water-enhanced multidetector CT enteroclysis. Radiology 2006; 241: 796-801.
[16] Putzer D, Gabriel M, Henninger B, Kendler D, Uprimny C, Dobrozemsky G, Decristoforo C, Bale RJ, Jaschke W and Virgolini IJ. Bone metastases in patients with neuroendocrine tumor: 68Ga-DOTA-Tyr3-octreotide PET in comparison to CT and bone scintigraphy. J Nucl Med 2009; 50: 1214-1221.
[17] Olson MC, Navin PJ, Welle CL and Goenka AH. Small bowel radiology. Curr Opin Gastroenterol 2021; 37: 267-274.
[18] Baumann T, Rottenburger C, Nicolas G and Wild D. Gastroenteropancreatic neuroendocrine tumours (GEP-NET) - Imaging and staging. Best Pract Res Clin Endocrinol Metab 2016; 30: 45-57.
[19] Yu R and Wachsman A. Imaging of neuroendocrine tumors: indications, interpretations, limits, and pitfalls. Endocrinol Metab Clin North Am 2017; 46: 795-814.
[20] Brenner R, Metens T, Bali M, Demetter P and Matos C. Pancreatic neuroendocrine tumor: added value of fusion of T2-weighted imaging and high b-value diffusion-weighted imaging for tumor detection. Eur J Radiol 2012; 81: e746-749.
[21] Dromain C, de Baere T, Lumbroso J, Caillet H, Laplanche A, Boige V, Ducreux M, Duvillard P, Elias D, Schlumberger M, Sigal R and Baudin E. Detection of liver metastases from endocrine tumors: a prospective comparison of somatostatin receptor scintigraphy, computed tomography, and magnetic resonance imaging. J Clin Oncol 2005; 23: 70-78.
[22] Sundin A. Radiological and nuclear medicine imaging of gastroenteropancreatic neuroendocrine tumours. Best Pract Res Clin Gastroenterol 2012; 26: 803-818.
[23] Mayerhoefer ME, Ba-Ssalamah A, Weber M, Mitterhauser M, Eidherr H, Wadsak W, Raderer M, Trattnig S, Herneth A and Karanikas G. Gadoxetate-enhanced versus diffusion-weighted MRI for fused Ga-68-DOTANOC PET/MRI in patients with neuroendocrine tumours of the upper abdomen. Eur Radiol 2013; 23: 1978-1985.
[24] Wild D, Schmitt JS, Ginj M, Mäcke HR, Bernard BF, Krenning E, De Jong M, Wenger S and Reubi JC. DOTA-NOC, a high-affinity ligand of somatostatin receptor subtypes 2, 3 and 5 for labelling with various radiometals. Eur J Nucl Med Mol Imaging 2003; 30: 1338-1347.
[25] Hofmann M, Maecke H, Börner R, Weckesser E, Schöffski P, Oei L, Schumacher J, Henze M, Heppeler A, Meyer J and Knapp H. Biokinetics and imaging with the somatostatin receptor PET radioligand (68)Ga-DOTATOC: preliminary data. Eur J Nucl Med 2001; 28: 1751-1757.
[26] Poletto G, Cecchin D, Sperti S, Filippi L, Realdon N and Evangelista L. Head-to-head comparison between peptide-based radiopharmaceutical for PET and SPECT in the evaluation of neuroendocrine tumors: a systematic review. Curr Issues Mol Biol 2022; 44: 5516-5530.

[27] Bozkurt MF, Virgolini I, Balogova S, Beheshti M, Rubello D, Decristoforo C, Ambrosini V, Kjaer A, Delgado-Bolton R, Kunikowska J, Oyen WJG, Chiti A, Giammarile F, Sundin A and Fanti S. Guideline for PET/CT imaging of neuroendocrine neoplasms with (68)Ga-DOTA-conjugated somatostatin receptor targeting peptides and (18)F-DOPA. Eur J Nucl Med Mol Imaging 2017; 44: 1588-1601.

[28] Antunes P, Ginj M, Zhang H, Waser B, Baum RP, Reubi JC and Maecke H. Are radiogallium-labelled DOTA-conjugated somatostatin analogues superior to those labelled with other radiometals? Eur J Nucl Med Mol Imaging 2007; 34: 982-993.

[29] Yadav D, Ballal S, Yadav MP, Tripathi M, Roesch F and Bal C. Evaluation of [(68)Ga]Ga-DATA-TOC for imaging of neuroendocrine tumours: comparison with [(68)Ga]Ga-DOTA-NOC PET/CT. Eur J Nucl Med Mol Imaging 2020; 47: 860-869.

[30] Poeppel TD, Binse I, Petersenn S, Lahner H, Schott M, Antoch G, Brandau W, Bockisch A and Boy C. 68Ga-DOTATOC versus 68Ga-DOTATATE PET/CT in functional imaging of neuroendocrine tumors. J Nucl Med 2011; 52: 1864-1870.

[31] Treglia G, Sadeghi R, Giovinazzo F, Galiandro F, Annunziata S, Muoio B and Kroiss AS. PET with different radiopharmaceuticals in neuroendocrine neoplasms: an umbrella review of published meta-analyses. Cancers (Basel) 2021; 13: 5172.

[32] Milione M, Maisonneuve P, Spada F, Pellegrinelli A, Spaggiari P, Albarello L, Pisa E, Barberis M, Vanoli A, Buzzoni R, Pusceddu S, Concas L, Sessa F, Solcia E, Capella C, Fazio N and La Rosa S. The clinicopathologic heterogeneity of Grade 3 gastroenteropancreatic neuroendocrine neoplasms: morphological differentiation and proliferation identify different prognostic categories. Neuroendocrinology 2017; 104: 85-93.

[33] Pauwels E, Cleeren F, Bormans G and Deroose CM. Somatostatin receptor PET ligands - the next generation for clinical practice. Am J Nucl Med Mol Imaging 2018; 8: 311-331.

[34] Ginj M, Zhang H, Waser B, Cescato R, Wild D, Wang X, Erchegyi J, Rivier J, Mäcke HR and Reubi JC. Radiolabeled somatostatin receptor antagonists are preferable to agonists for in vivo peptide receptor targeting of tumors. Proc Natl Acad Sci U S A 2006; 103: 16436-16441.

[35] Fani M, Nicolas GP and Wild D. Somatostatin receptor antagonists for imaging and therapy. J Nucl Med 2017; 58 Suppl 2: 61S-66S.

[36] Nicolas GP, Beykan S, Bouterfa H, Kaufmann J, Bauman A, Lassmann M, Reubi JC, Rivier JEF, Maecke HR, Fani M and Wild D. Safety, biodistribution, and radiation dosimetry of (68)Ga-OPS202 in patients with gastroenteropancreatic neuroendocrine tumors: a prospective phase i imaging study. J Nucl Med 2018; 59: 909-914.

[37] Nicolas GP, Schreiter N, Kaul F, Uiters J, Bouterfa H, Kaufmann J, Erlanger TE, Cathomas R, Christ E, Fani M and Wild D. Sensitivity comparison of (68)Ga-OPS202 and (68)Ga-DOTATOC PET/CT in patients with gastroenteropancreatic neuroendocrine tumors: a prospective phase II imaging study. J Nucl Med 2018; 59: 915-921.

[38] Kanellopoulos P, Nock BA, Greifenstein L, Baum RP, Roesch F and Maina T. [(68)Ga]Ga-DATA(5m)-LM4, a PET radiotracer in the diagnosis of SST(2)R-positive tumors: preclinical and first clinical results. Int J Mol Sci 2022; 23: 14590.

[39] Viswanathan R, Ballal S, Yadav MP, Roesch F, Sheokand P, Satapathy S, Tripathi M, Agarwal S, Moon ES and Bal C. Head-to-head comparison of SSTR antagonist [(68)Ga]Ga-DATA(5m)-LM4 with SSTR agonist [(68)Ga]Ga-DOTANOC PET/CT in patients with well differentiated gastroenteropancreatic neuroendocrine tumors: a prospective imaging study. Pharmaceuticals (Basel) 2024; 17: 275.

[40] Liu M, Cheng Y, Bai C, Zhao H, Jia R, Chen J, Zhu W and Huo L. Gallium-68 labeled somatostatin receptor antagonist PET/CT in over 500 patients with neuroendocrine neoplasms: experience from a single center in China. Eur J Nucl Med Mol Imaging 2024; 51: 2002-2011.

[41] Zhu W, Jia R, Yang Q, Cheng Y, Zhao H, Bai C, Xu J, Yao S and Huo L. A prospective randomized, double-blind study to evaluate the diagnostic efficacy of (68)Ga-NODAGA-LM3 and (68)Ga-DOTA-LM3 in patients with well-differentiated neuroendocrine tumors: compared with (68)Ga-DOTATATE. Eur J Nucl Med Mol Imaging 2022; 49: 1613-1622.

[42] Zhu W, Cheng Y, Wang X, Yao S, Bai C, Zhao H, Jia R, Xu J and Huo L. Head-to-head comparison of (68)Ga-DOTA-JR11 and (68)Ga-DOTATATE PET/CT in patients with metastatic, well-differentiated neuroendocrine tumors: a prospective study. J Nucl Med 2020; 61: 897-903.

[43] Kaemmerer D, Träger T, Hoffmeister M, Sipos B, Hommann M, Sänger J, Schulz S and Lupp A. Inverse expression of somatostatin and CXCR4 chemokine receptors in gastroenteropancreatic neuroendocrine neoplasms of different malignancy. Oncotarget 2015; 6: 27566-27579.

[44] Guembarovski AL, Guembarovski RL, Hirata BKB, Vitiello GAF, Suzuki KM, Enokida MT, Watanabe MAE and Reiche EMV. CXCL12 chemokine and CXCR4 receptor: association with susceptibility and prognostic markers in triple negative breast cancer. Mol Biol Rep 2018; 45: 741-750.

[45] Yin X, Liu Z, Zhu P, Wang Y, Ren Q, Chen H and Xu J. CXCL12/CXCR4 promotes proliferation, migration, and invasion of adamantinomatous craniopharyngiomas via PI3K/AKT signal pathway. J Cell Biochem 2019; 120: 9724-9736.

[46] Werner RA, Weich A, Higuchi T, Schmid JS, Schirbel A, Lassmann M, Wild V, Rudelius M, Kudlich T, Herrmann K, Scheurlen M, Buck AK, Kropf S, Wester HJ and Lapa C. Imaging of chemokine receptor 4 expression in neuroendocrine tumors - a triple tracer comparative approach. Theranostics 2017; 7: 1489-1498.

[47] Weich A, Werner RA, Buck AK, Hartrampf PE, Serfling SE, Scheurlen M, Wester HJ, Meining A, Kircher S, Higuchi T, Pomper MG, Rowe SP, Lapa C and Kircher M. CXCR4-directed PET/CT in patients with newly diagnosed neuroendocrine carcinomas. Diagnostics (Basel) 2021; 11: 605.

[48] Mai R, Kaemmerer D, Träger T, Neubauer E, Sänger J, Baum RP, Schulz S and Lupp A. Different somatostatin and CXCR4 chemokine receptor expression in gastroenteropancreatic neuroendocrine neoplasms depending on their origin. Sci Rep 2019; 9: 4339.

[49] Michalski K, Schlötelburg W, Hartrampf P, Heinrich M, Serfling S, Buck AK, Werner RA, Kosmala A and Weich A. Volumetric parameters derived from CXCR4-directed PET/CT predict outcome in patients with gastrointestinal neuroendocrine carcinomas. Mol Imaging Biol 2024; 26: 344-350.

[50] Pang C, Li Y, Shi M, Fan Z, Gao X, Meng Y, Liu S, Gao C, Su P, Wang X and Zhan H. Expression and clinical value of CXCR4 in high grade gastroenteropancreatic neuroendocrine neoplasms. Front Endocrinol (Lausanne) 2024; 15: 1281622.

[51] Conti M and Eriksson L. Physics of pure and non-pure positron emitters for PET: a review and a discussion. EJNMMI Phys 2016; 3: 8.
[52] Pfeifer A, Knigge U, Mortensen J, Oturai P, Berthelsen AK, Loft A, Binderup T, Rasmussen P, Elema D, Klausen TL, Holm S, von Benzon E, Højgaard L and Kjaer A. Clinical PET of neuroendocrine tumors using 64Cu-DOTATATE: first-in-humans study. J Nucl Med 2012; 53: 1207-1215.
[53] Pfeifer A, Knigge U, Binderup T, Mortensen J, Oturai P, Loft A, Berthelsen AK, Langer SW, Rasmussen P, Elema D, von Benzon E, Højgaard L and Kjaer A. 64Cu-DOTATATE PET for neuroendocrine tumors: a prospective head-to-head comparison with 111In-DTPA-octreotide in 112 patients. J Nucl Med 2015; 56: 847-854.
[54] Johnbeck CB, Knigge U, Loft A, Berthelsen AK, Mortensen J, Oturai P, Langer SW, Elema DR and Kjaer A. Head-to-head comparison of (64)Cu-DOTATATE and (68)Ga-DOTATOC PET/CT: a prospective study of 59 patients with neuroendocrine tumors. J Nucl Med 2017; 58: 451-457.
[55] Loft M, Carlsen EA, Johnbeck CB, Johannesen HH, Binderup T, Pfeifer A, Mortensen J, Oturai P, Loft A, Berthelsen AK, Langer SW, Knigge U and Kjaer A. (64)Cu-DOTATATE PET in patients with neuroendocrine neoplasms: prospective, head-to-head comparison of imaging at 1 hour and 3 hours after injection. J Nucl Med 2021; 62: 73-80.
[56] Loft M, Carlsen EA, Johnbeck CB, Jensen CV, Andersen FL, Langer SW, Oturai P, Knigge U and Kjaer A. Activity dose reduction in (64)Cu-DOTATATE PET in patients with neuroendocrine neoplasms: impact on image quality and lesion detection ability. Mol Imaging Biol 2022; 24: 600-611.
[57] Liu X, Li N, Jiang T, Xu H, Ran Q, Shu Z, Wu J, Li Y, Zhou S and Zhang B. Comparison of gallium-68 somatostatin receptor and (18)F-fluorodeoxyglucose positron emission tomography in the diagnosis of neuroendocrine tumours: a systematic review and meta-analysis. Hell J Nucl Med 2020; 23: 188-200.
[58] Hicks RJ, Jackson P, Kong G, Ware RE, Hofman MS, Pattison DA, Akhurst TA, Drummond E, Roselt P, Callahan J, Price R, Jeffery CM, Hong E, Noonan W, Herschtal A, Hicks LJ, Hedt A, Harris M, Paterson BM and Donnelly PS. (64)Cu-SARTATE PET imaging of patients with neuroendocrine tumors demonstrates high tumor uptake and retention, potentially allowing prospective dosimetry for peptide receptor radionuclide therapy. J Nucl Med 2019; 60: 777-785.
[59] Laffon E, de Clermont H and Marthan R. An abbreviated therapy-dosimetric equation for the companion diagnostic/therapeutic [(64/67)Cu]Cu-SARTATE. EJNMMI Res 2021; 11: 75.
[60] Hope TA, Bergsland EK, Bozkurt MF, Graham M, Heaney AP, Herrmann K, Howe JR, Kulke MH, Kunz PL, Mailman J, May L, Metz DC, Millo C, O'Dorisio S, Reidy-Lagunes DL, Soulen MC and Strosberg JR. Appropriate use criteria for somatostatin receptor PET imaging in neuroendocrine tumors. J Nucl Med 2018; 59: 66-74.
[61] Han S, Lee HS, Woo S, Kim TH, Yoo C, Ryoo BY and Ryu JS. Prognostic value of 18F-FDG PET in neuroendocrine neoplasm: a systematic review and meta-analysis. Clin Nucl Med 2021; 46: 723-731.
[62] Chan DL, Pavlakis N, Schembri GP, Bernard EJ, Hsiao E, Hayes A, Barnes T, Diakos C, Khasraw M, Samra J, Eslick E, Roach PJ, Engel A, Clarke SJ and Bailey DL. Dual somatostatin receptor/FDG PET/CT imaging in metastatic neuroendocrine tumours: proposal for a novel grading scheme with prognostic significance. Theranostics 2017; 7: 1149-1158.
[63] Chan DL, Hayes AR, Karfis I, Conner A, Mileva M, Bernard E, Schembri G, Navalkissoor S, Gnanasegaran G, Pavlakis N, Marin C, Vanderlinden B, Flamen P, Roach P, Caplin ME, Toumpanakis C and Bailey DL. [(18)F]FDG PET/CT-avid discordant volume as a biomarker in patients with gastroenteropancreatic neuroendocrine neoplasms: a multicenter study. J Nucl Med 2024; 65: 185-191.
[64] Dubash SR, Keat N, Mapelli P, Twyman F, Carroll L, Kozlowski K, Al-Nahhas A, Saleem A, Huiban M, Janisch R, Frilling A, Sharma R and Aboagye EO. Clinical translation of a click-labeled 18F-octreotate radioligand for imaging neuroendocrine tumors. J Nucl Med 2016; 57: 1207-1213.
[65] Meisetschläger G, Poethko T, Stahl A, Wolf I, Scheidhauer K, Schottelius M, Herz M, Wester HJ and Schwaiger M. Gluc-Lys([18F]FP)-TOCA PET in patients with SSTR-positive tumors: biodistribution and diagnostic evaluation compared with [111In]DTPA-octreotide. J Nucl Med 2006; 47: 566-573.
[66] Dubash S, Barwick TD, Kozlowski K, Rockall AG, Khan S, Khan S, Yusuf S, Lamarca A, Valle JW, Hubner RA, McNamara MG, Frilling A, Tan T, Wernig F, Todd J, Meeran K, Pratap B, Azeem S, Huiban M, Keat N, Lozano-Kuehne JP, Aboagye EO and Sharma R. Somatostatin receptor imaging with [(18)F]FET-βAG-TOCA PET/CT and [(68)Ga]Ga-DOTA-peptide PET/CT in patients with neuroendocrine tumors: a prospective, phase 2 comparative study. J Nucl Med 2024; 65: 416-422.
[67] Wängler C, Beyer L, Bartenstein P, Wängler B, Schirrmacher R and Lindner S. Favorable SSTR subtype selectivity of SiTATE: new momentum for clinical [(18)F]SiTATE PET. EJNMMI Radiopharm Chem 2022; 7: 22.
[68] Ilhan H, Todica A, Lindner S, Boening G, Gosewisch A, Wängler C, Wängler B, Schirrmacher R and Bartenstein P. First-in-human (18)F-SiFAlin-TATE PET/CT for NET imaging and theranostics. Eur J Nucl Med Mol Imaging 2019; 46: 2400-2401.
[69] Ilhan H, Lindner S, Todica A, Cyran CC, Tiling R, Auernhammer CJ, Spitzweg C, Boeck S, Unterrainer M, Gildehaus FJ, Böning G, Jurkschat K, Wängler C, Wängler B, Schirrmacher R and Bartenstein P. Biodistribution and first clinical results of (18)F-SiFAlin-TATE PET: a novel (18)F-labeled somatostatin analog for imaging of neuroendocrine tumors. Eur J Nucl Med Mol Imaging 2020; 47: 870-880.
[70] Beyer L, Gosewisch A, Lindner S, Völter F, Mittlmeier LM, Tiling R, Brendel M, Cyran CC, Unterrainer M, Rübenthaler J, Auernhammer CJ, Spitzweg C, Böning G, Gildehaus FJ, Jurkschat K, Wängler C, Wängler B, Schirrmacher R, Wenter V, Todica A, Bartenstein P and Ilhan H. Dosimetry and optimal scan time of [(18)F]SiTATE-PET/CT in patients with neuroendocrine tumours. Eur J Nucl Med Mol Imaging 2021; 48: 3571-3581.
[71] Eschbach RS, Hofmann M, Späth L, Sheikh GT, Delker A, Lindner S, Jurkschat K, Wängler C, Wängler B, Schirrmacher R, Tiling R, Brendel M, Wenter V, Dekorsy FJ, Zacherl MJ, Todica A, Ilhan H, Grawe F, Cyran CC, Unterrainer M, Rübenthaler J, Knösel T, Paul T, Boeck S, Westphalen CB, Spitzweg C, Auernhammer CJ, Bartenstein P, Unterrainer LM and Beyer L. Comparison of somatostatin receptor expression in patients with neuroendocrine tumours with

and without somatostatin analogue treatment imaged with [(18)F]SiTATE. Front Oncol 2023; 13: 992316.

[72] Pauwels E, Cleeren F, Tshibangu T, Koole M, Serdons K, Dekervel J, Van Cutsem E, Verslype C, Van Laere K, Bormans G and Deroose CM. Al(18)F-NOTA-octreotide: first comparison with (68)Ga-DOTATATE in a neuroendocrine tumour patient. Eur J Nucl Med Mol Imaging 2019; 46: 2398-2399.

[73] Long T, Yang N, Zhou M, Chen D, Li Y, Li J, Tang Y, Liu Z, Li Z and Hu S. Clinical application of 18F-AlF-NOTA-octreotide PET/CT in combination with 18F-FDG PET/CT for imaging neuroendocrine neoplasms. Clin Nucl Med 2019; 44: 452-458.

[74] Pauwels E, Cleeren F, Tshibangu T, Koole M, Serdons K, Boeckxstaens L, Dekervel J, Vandamme T, Lybaert W, den Broeck BV, Laenen A, Clement PM, Geboes K, Cutsem EV, Stroobants S, Verslype C, Bormans G and Deroose CM. (18)F-AlF-NOTA-octreotide outperforms (68)Ga-DOTATATE/NOC PET in neuroendocrine tumor patients: results from a prospective, multicenter study. J Nucl Med 2023; 64: 632-638.

[75] Hou J, Long T, Yang N, Chen D, Zeng S, Zheng K, Liao G and Hu S. Biodistribution of (18)F-AlF-NOTA-octreotide in different organs and characterization of uptake in neuroendocrine neoplasms. Mol Imaging Biol 2021; 23: 827-835.

[76] Hofman MS, Lau WF and Hicks RJ. Somatostatin receptor imaging with 68Ga DOTATATE PET/CT: clinical utility, normal patterns, pearls, and pitfalls in interpretation. Radiographics 2015; 35: 500-516.

[77] Xie Q, Liu T, Ding J, Zhou N, Meng X, Zhu H, Li N, Yu J and Yang Z. Synthesis, preclinical evaluation, and a pilot clinical imaging study of [(18)F]AlF-NOTA-JR11 for neuroendocrine neoplasms compared with [(68)Ga]Ga-DOTA-TATE. Eur J Nucl Med Mol Imaging 2021; 48: 3129-3140.

[78] Ahenkorah S, Cawthorne C, Murce E, Deroose CM, Cardinaels T, Seimbille Y, Bormans G, Ooms M and Cleeren F. Direct comparison of [(18)F]AlF-NOTA-JR11 and [(18)F]AlF-NOTA-octreotide for PET imaging of neuroendocrine tumors: antagonist versus agonist. Nucl Med Biol 2023; 118-119: 108338.

[79] Pandit-Taskar N, Zanzonico P, Staton KD, Carrasquillo JA, Reidy-Lagunes D, Lyashchenko S, Burnazi E, Zhang H, Lewis JS, Blasberg R, Larson SM, Weber WA and Modak S. Biodistribution and dosimetry of (18)F-meta-fluorobenzylguanidine: a first-in-human PET/CT imaging study of patients with neuroendocrine malignancies. J Nucl Med 2018; 59: 147-153.

[80] Samim A, Tytgat GAM, Bleeker G, Wenker STM, Chatalic KLS, Poot AJ, Tolboom N, van Noesel MM, Lam MGEH and de Keizer B. Nuclear medicine imaging in neuroblastoma: current status and new developments. J Pers Med 2021; 11: 270.

[81] Wang P, Li T, Cui Y, Zhuang H, Li F, Tong A and Jing H. 18 F-MFBG PET/CT is an effective alternative of 68 Ga-DOTATATE PET/CT in the evaluation of metastatic pheochromocytoma and paraganglioma. Clin Nucl Med 2023; 48: 43-48.

[82] Chen W, Silverman DH, Delaloye S, Czernin J, Kamdar N, Pope W, Satyamurthy N, Schiepers C and Cloughesy T. 18F-FDOPA PET imaging of brain tumors: comparison study with 18F-FDG PET and evaluation of diagnostic accuracy. J Nucl Med 2006; 47: 904-911.

[83] Nölting S, Bechmann N, Taieb D, Beuschlein F, Fassnacht M, Kroiss M, Eisenhofer G, Grossman A and Pacak K. Personalized management of pheochromocytoma and paraganglioma. Endocr Rev 2022; 43: 199-239.

[84] Sung C, Lee HS, Lee DY, Kim YI, Kim JE, Lee SJ, Oh SJ, Sung TY, Lee YM, Kim YH, Kim BJ, Koh JM, Lee SH and Ryu JS. A prospective comparative study of 18 F-FDOPA PET/CT versus 123 I-MIBG scintigraphy with SPECT/CT for the diagnosis of pheochromocytoma and paraganglioma. Clin Nucl Med 2024; 49: 27-36.

[85] He Q, Zhang Z, Zhang L, Zhang B, Long Y, Zhang Y, Liao Z, Zha Z and Zhang X. Head-to-head comparison between [(68)Ga]Ga-DOTA-NOC and [(18)F]DOPA PET/CT in a diverse cohort of patients with pheochromocytomas and paragangliomas. Eur J Nucl Med Mol Imaging 2024; 51: 1989-2001.